Strain-induced Self-rolling III-V Tubular nanostructures: Formation Process and Photonic Applications

Ik Su Chun,[1] Kevin Bassett,[1] Archana Challa,[1] Xin Miao,[1] and Mika Saarinen[2], Xiuling Li[1*]

[1]Department of Electrical and Computer Engineering, University of Illinois, Urbana, IL 61801
[2]Optoelectronics Research Centre, Tampere University of Technology, Tampere, Finland
* xiuling@illinois.edu

ABSTRACT

We demonstrate the rolling process of strained III-V compound semiconductor films upon epitaxial liftoff from the substrate. The formed tubular structures with diameters in the micron range, embedded with quantum confined GaAs light emitters in the ultra-thin tube walls (< 100 nm) show dramatic enhancement in intensity and reduction of bandgap as a function of tube curvature. Emission characteristics and implications are analyzed.

1. INTRODUCTION

Strain induced self rolled-up semiconductor tubes is a new nanotechnology paradigm. They are formed spontaneously through the mechanism of strain relaxation after releasing pseudomorphically strained epitaxial films from their native substrate. Figure 1 illustrates an example of such self-rolling phenomenon using a GaAs-$In_xGa_{1-x}As$ bilayer system as an example, where the $In_xGa_{1-x}As$ layer is compressively strained relative to GaAs. Upon releasing the GaAs- $In_xGa_{1-x}As$ bilayer from the substrate by selectively removing the AlAs sacrificial layer, the strained bilayer curves up and starts rolling as the sacrificial layer is etched laterally.

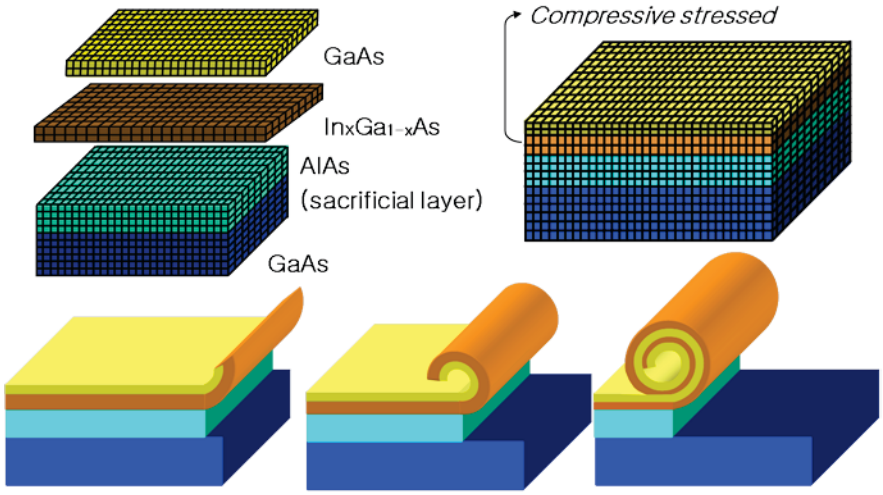

Figure 1 Mechanism of strain induced self-rolling of semiconductor micro and nanotubes. Schematic illustration of the formation of GaAs-$In_xGa_{1-x}As$ tubes from pseudomorphically grown epitaxial films to the liftoff releasing process by selectively removing the AlAs sacrificial layer. The epitaxial growth with defined thickness and mismatch strain is the bottom up aspect that determines the tube diameter, and the liftoff releasing process is the top-down side that enables positioning and alignment control of these tubes.

*all correspondence should be addressed to: xiuling@illinois.edu

Quantum Sensing and Nanophotonic Devices VII, edited by Manijeh Razeghi, Rengarajan Sudharsanan, Gail J. Brown,
Proc. of SPIE Vol. 7608, 760810 · © 2010 SPIE · CCC code: 0277-786X/10/$18 · doi: 10.1117/12.844046

In contrast to the so called pure "bottom-up" growth and "top-down" fabrication approaches for nanotechnology, the formation of self-rolling semiconductor micro and nanotubes employs both. The "bottom-up" growth approach usually replies on self-assembly at the molecular level to form nanostructures of different size and shape as a result of energy minimization under the given growth condition and environment. Nanostructures as small as 1 nm can be synthesized using the bottom-up method. However, the sensitive or responsive nature of self-assembly makes the nanostructure size and shape uniformity as well site control a challenge for practical applications. On the other hand, the "top-down" fabrication approach uses modern lithography patterning methods and subsequent etching to define the nanostructure feature size and location by removing the unwanted part of the materials from the top-down. As a result, the lateral resolution is defined by the lithography technology, and the depth (aspect ratio) is a function of sidewall verticalness under the specified etching condition. The "subtraction" nature of the top-down approach also makes it prone to sidewall damages due to the etching process.

Table I. Comparison of top-down and bottom-up formation of nanostructures.

Nanostructure formation	Bottom-up self-assembly	Top-down fabrication
Size control	Not limited by lithography resolution	Limited by lithography resolution
Size uniformity control	Lacking	Good
Site control	Lacking	Good
Processing damage	None	Etching induced damage

The rolled-up semiconductor tubes are formed by the combination of bottom-up and top down approaches. The bottom up aspect is the epitaxial growth of the strained layers with the desired composition and thickness, which determines the tube diameter. The top-down aspect is the definition of the mesa for the lateral etching of the sacrificial layer in order to release the strained layer from the substrate. This mesa controls the ultimate tube location, dimension (length and width), number of rotations, and direction (relative to crystal orientation), but not the inner diameter. *As a result, self-rolling tubular nanostructures with precise spatial location and alignment control can be formed.*[1]

2. FORMATION PROCESS

Metalorganic Chemical Vapor Deposition (MOCVD) and Molecular Beam Epitaxy (MBE) are used to grow the arsenide based III-V epitaxial films. The self-rolling process is essentially an epitaxial liftoff process, except the liftoff involves rolling into the 3rd dimension introducing another degree of freedom "curvature" for nanostructures. There are two essential components in the strain induced self-rolling of semiconductors: sacrificial layer that can release the film from the substrate, and net strain in the epitaxial film to be released. The most common sacrificial layer that can be selectively removed from GaAs is $Al_xGa_{1-x}As$ using HF solution. $In_xGa_{1-x}P$ is another possible sacrificial layer that can be removed selectively from As-based materials (except high Al% $Al_xGa_{1-x}As$) using HCl solution.

2.1 Diameter dependence of semiconductor rolled-up micro and nanotubes

The diameter dependence of the self-rolled-up tubes can be described semi-quantitatively by a classical continuum theory that considers the film thickness, mismatch strain and stiffness (Young's modulus), as described in Equation 1 below. Obviously, the diameter is proportional to total thickness and inversely proportional to mismatch strain. However, thickness ratio also matters. For materials with similar Young's moduli, Equation 1 can be simplified to $D=(d_1+d_2)^3/3\varepsilon d_1 d_2$. As reported before[2], the experimentally measured tube diameter is 15-20% smaller than calculated using the continuum model. For a typical thickness and mismatch strain for III-V materials system, assuming the mismatch strain is 1% to 7%, and total film thickness of 1 nm to 100 nm, the tube diameter would be in the range of 10 nm – 10 μm. The smallest tube that can be formed with III-As materials system is ~ 3 nm with 1 ML of InAs and 1 ML of GaAs which has a mismatch strain of 7.16%.

$$D = \frac{d[\,3(1+m)^2 + (1+m\cdot n)\cdot[m^2+(m\cdot n)^{-1}]]}{3\varepsilon(1+m)^2}$$

- $d = d_1+d_2$: the total thickness of the bilayers
- ε : the in-plane biaxial strain between the two layers
  - → introduced due to the lattice mismatch between the two layers
- $n = Y_1/Y_2$: the ratio of Young's modules
- $m = d_1/d_2$: the raitio of the thickness of the first and second layer

2.2 Crystal orientation dependence

It has been unambiguously proved that <001> is the preferred rolling direction due to Young's Modulus anisotropy in cubic crystals.[3] As shown in Table I, the minimum Young's modulus value is <001> direction while the maximum value is <111> for all common cubic semiconductor crystals.

Table 2 Summary of Young's modulus values (GPa) from literature[4]

Material	<001>	<011>	<111>
GaAs	85.3	121.3	141.2
GaP	103.4	144.7	166.9
Si	130.2	168.9	187.5
Ge	103.7	138.0	155.1

This is a very useful property that can be employed to roll-up, bent-over, and twist-up membranes from edges, corners to form MEMS/NEMS structures that are more versatile than what silicon thin films could offer. This aspect of the strain induced self-rolling phenomenon has been nicely reviewed recently by Prinz et al.[5]

2.3 Geometry dependence for semiconductor rolled-up micro and nanotubes

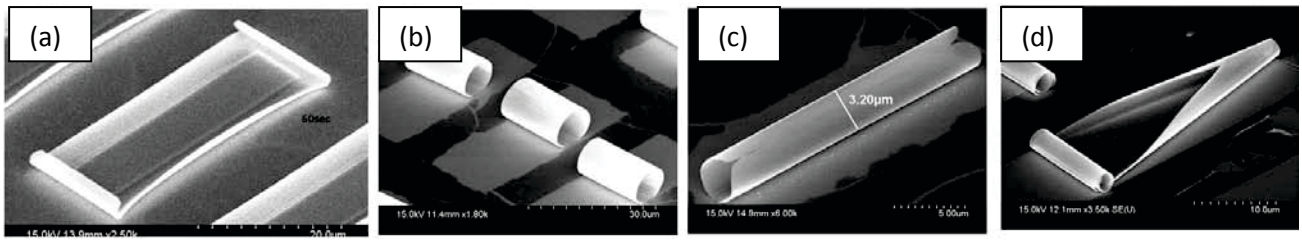

Figure 2 Geometry dependence of semiconductor micro and nanotube formation. SEM images show (from left to right) the initial stage of liftoff where all four sides of the rectangular mesa start to roll-up; the short-side rolling tubes; the long-side rolling tubes; and the tubes that rolled up from both sides simultaneously. Both the rectangular mesa dimensions as well as the diameters of the tubes affect the rolling direction, which is a result of energy minimization.

One way to release the strained film from the substrate is to lithographically pattern rectangular mesa stripes to expose the sidewalls thus sacrificial layer for lateral etching. We have found that the same mesa stripe geometry with the sides oriented along <100> (the soft direction) could result in tubes with different length and different number of rotations, depending on which one of the crystallographically equivalent <100> directions the tubes roll from. Figure 2a shows the initial rolling stage for rectangular strip geometry of a GaAs-$In_xGa_{1-x}As$ bilayer film where all four sides start to curve up. Depending on the actual dimension of the rectangular mesa, the tube diameter, the lateral etching anisotropy, and certain kinetic variations, rolling could end up occurring from the short side (Figure 2b), or long side (Figure 2c); or both directions (Figure 2d). Clearly it is critical to be able to understand and control the rolling direction in order to design tubes with the desired length and number of rotations. The detailed results will be reported separately which includes simulations on the lowest energy state as a function of releasing stage with various geometries.

2.4 Patterned rolled-up tubes

The details of the tube geometry including the edge smoothness, intentionally created bottle-like notches, and periodic undulations have been reported to lead directional emission or better confinement.[6-8] We have studied rolled-up tubes using membranes not only with patterns at the edges but also throughout the entire membranes. Shown in Figure 3 are tubes formed from patterned membrane with periodic arrays of holes. These holes not only serve as etching holes for faster release, but also add to the functionality of the tubes, e.g. with proper design, the holes can be lined up after rolling for unique 3D photonic crystal structures. Note that the patterning on the rolled-up membranes showed no change on the tube diameter.

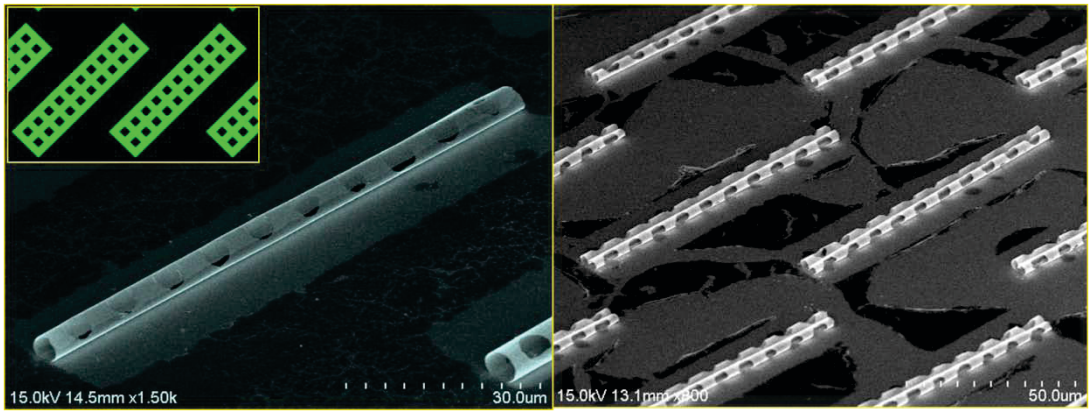

Figure 3 Holey tubes formed from patterned membranes. SEM image of holey tubes formed using 20 μm x 105 μm strained membranes patterned with an arrays of 5 x 5 μm^2 holes. The tube diameter shows negligible change compared to solid membrane of the same materials.

3 FUNCTIONAL ROLLED-UP TUBES FOR OPTOELECTRONICS

In the previous examples, the rolled-up membrane mostly consists of a simple bilayer that is lattice mismatched relative to each other. In this section, we will focus on the functions of rolled-up tubes with active quantum confined light emitting structures embedded in the tube walls.

3.1 Incorporating active light emitting layers in the tube wall: quantum well, dots, and wires

Illustrated in Figure 4 are three different types of active structures that can be rolled up by using the strained $In_xGa_{1-x}As$ layer as a wrapper while keeping the rest of the layers either lattice matched to the substrate (GaAs quantum well) or involving discrete structures (quantum dots and nanowires). On both sides of the active layers, there are 10 nm thick $Al_{0.33}Ga_{0.67}As$ barrier layers for electronic and optical confinement. The film growth for the quantum well and quantum dot structures is straightforward as in the growth of planar laser structures, except the design involves much thinner layers. The growth of the nanowire structure on the other hand takes a special regrowth process that includes three temperature steps, where the planar nanowire growth is catalyzed by Au colloids and formed through the vapor-liquid-solid mechanism; and the barrier layers are formed in situ taking advantage of the high Au mobility at high growth temperature.[9] The initial growth stops after the $In_xGa_{1-x}As$ strained layer, followed by the external deposition/patterning of Au colloids, which then return to the MOCVD growth chamber for a three-step regrowth that results in sandwiching the planar GaAs nanowires epitaxially inbetween $Al_{0.33}Ga_{0.67}As$ barriers.[9] The three-step growth starts with a high temperature step (625°C) where the epitaxial growth of $Al_{0.33}Ga_{0.67}As$ barrier takes place underneath the Au colloids which simply elevate to the surface at this temperature, followed by a low temperature (465°C) step where self-aligned planar nanowires form. After the nanowire growth, high growth temperature (625°C) is again used for the growth of top $Al_{0.33}Ga_{0.67}As$ barrier and GaAs cap while keeping the Au colloids elevated at the surface. Au colloids can be subsequently removed before rolling up the strained films. In this article, we focus on the optical properties of the rolled-up quantum well tubes.

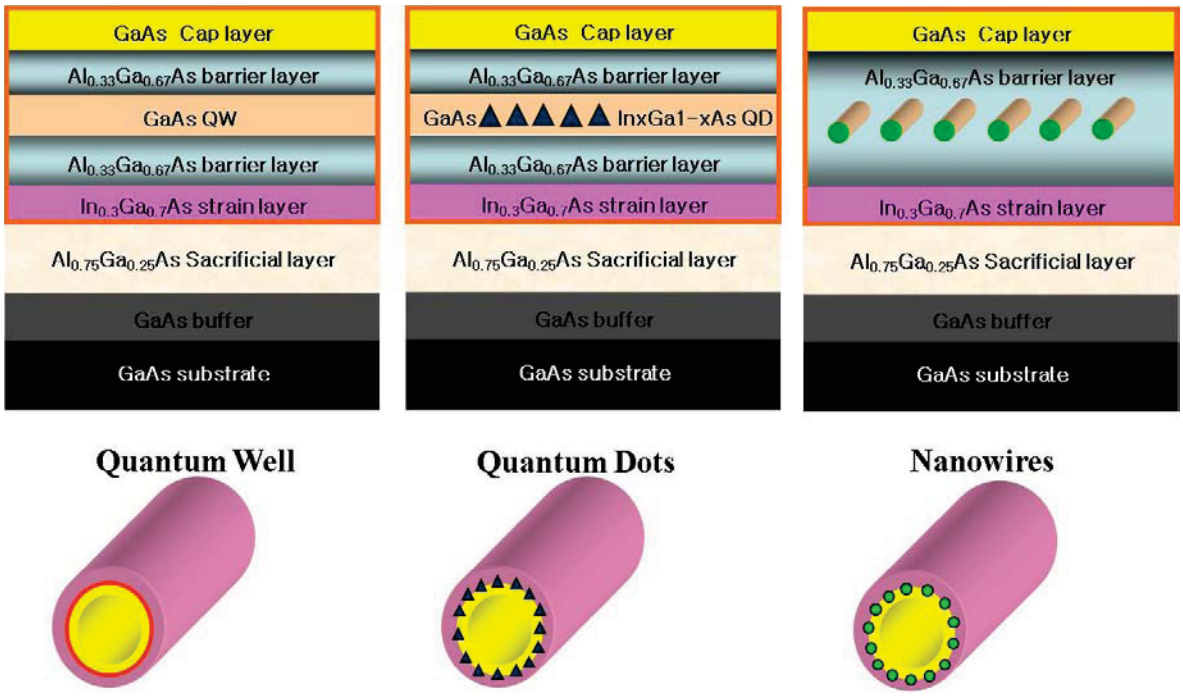

Figure 4 Illustration of the epitaxial structures (before rolling) of three types of quantum confined light emitters embedded in the tube wall of self-rolling semiconductor micro and nanotubes. From left to right: GaAs QW tube, $In_xGa_{1-x}As$ QD tube, and GaAs nanowire tube.

3.2 Optical properties of rolled-up light emitting structures: quantum well tubes

Figure 5 (top) shows a schematic of the conduction band edge structure (no band bending incorporated) of an epitaxial film, consisting of a 5 nm GaAs quantum well cladded by 10 nm $Al_{0.33}Ga_{0.67}As$ layers on both sides and supported by a strained InGaAs layer which will wrap up the quantum well stack once released from the substrate (AlAs sacrificial layer between InGaAs and substrate is not drawn). We have performed room temperature photoluminescence (PL) study as a function of tube curvature, laser pumping power, as well as polarization. In all cases, the active region is a 5 nm GaAs layer cladded by 10 nm $Al_{0.33}Ga_{0.67}As$ layers on both sides. The strained InGaAs layer composition and thickness, and the GaAs cap thickness are adjusted to change the tube curvature. As shown in Figure 5 (bottom), before the film is released from the substrate, the PL taken at room temperature using a 532 nm Nd:YAG laser with a spot size of 50 μm, is dominated by emission from bulk GaAs substrate, which appears at 862 nm at low pump power (1 mW) and monotonically shifts to longer wavelength with increasing power and reaches 881 nm at 90 mW. The peak at ~ 1020 nm, visible at low pump power (1 mW) and saturates at higher pump power, probably originates from the InGaAs layer. Not surprisingly, the GaAs QW peak (blue shift from the bulk peak due to quantum confinement) is not observed at all, probably due to insufficient optical confinement from the ultra-thin (20 nm) $Al_{0.33}Ga_{0.67}As$ barriers and the strong absorption from the substrate.

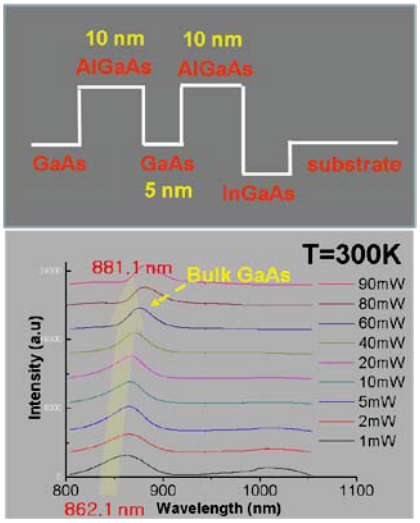

Figure 5 Structure and PL of the GaAs QW film before releasing from the substrate. Pump laser is 532 nm and spot size is ~ 50 um.

To evaluate the effect of substrate absorption, we have released the planar GaAs QW stack in stripe geometry without the InGaAs strained layer (Figure 6 left) and dispersed onto a transparent (sapphire) substrate. A weak PL peak at 817 nm is now observed when PL is taken from a cluster of the membrane stripes, consistent with bandgap enlargement due to quantum confinement in the 5 nm GaAs QW. Removing the native substrate and associated absorption indeed enhances the QW emission in this case.

The PL intensity from the QW is further enhanced dramatically once the planar membrane is rolled up along with the InGaAs strained layer. Shown in Figure 6 (right) are the structure, a SEM image of a single tube that is 3 um in diameter and 2.5 rotations and the micro-PL spectrum taken from the single tube on a sapphire substrate. A strong and distinct peak at 834 nm is clearly observed for a single tube that is 38 nm in each rotation of the wall thickness. The intensity enhancement observed here is consistent with other reports for rolled-up quantum dot and quantum well tubes and other curved/wrinkled structures.[10-12] Several mechanisms have been proposed to explain the intensity enhancement including interference contrast theory and better optical confinement.[11]

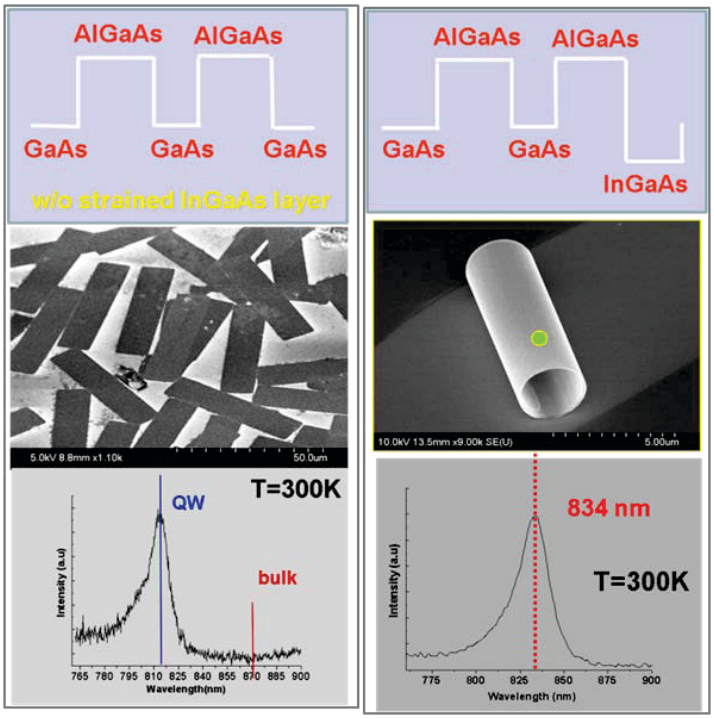

Figure 6 Planar (left) and rolled-up (right) GaAs QW membrane structure, SEM image, and micro-PL spectra.

Shown in Figure 7 is the PL intensity comparison between the holey membrane tubes in Figure 3 and the solid membrane tubes and solid planar membranes. Note that all three structures were fabricated from the same size stripes of the same epitaxial material (except the planar membrane does not have the InGaAs layer). It can be seen that the loss of materials in the holey tubes not only did not lead to a decrease in PL intensity but to the contrary, a clear intensity enhancement, presumably due to the high contrast of index of refraction for the materials around the air holes. This observation confirms that better optical confinement due to larger index contrast is the origin of the PL intensity enhancement for rolled-up structures.

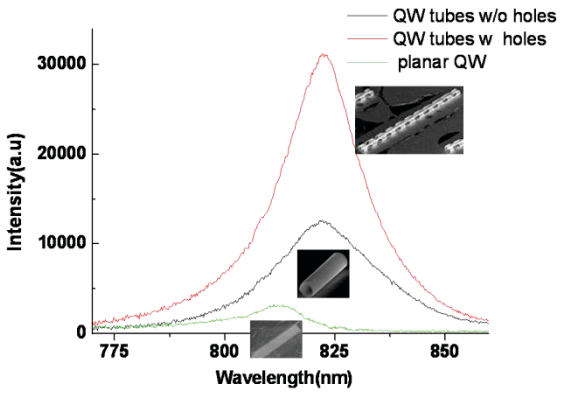

Figure 7 PL spectra from three categories (from the same size stripes) of GaAs QW structures (planar, rolled-up, and rolled-up with holes) on sapphire substrate. Intensity enhancement of more than 10x can be seen in the holey tubes compared to the planar membrane.

In an attempt to achieve optically pumped lasing, we have done a power dependence study of the rolled-up QW tubes. Shown in Figure 8 is an example of pumping a cluster of QW tubes that are stacked on top of each other randomly on a sapphire substrate. A monotonic increase in intensity is observed in the power range from 2 to 70 mW before it reaches saturation. The peak shift as a function of power shows slight red shift with increasing power before reaching the plateau. It is remarkable that strong room temperature PL can be observed from films as thin as 30 nm, however, no mode-like peaks or peak narrowing was observed for the power range studied for this structure.

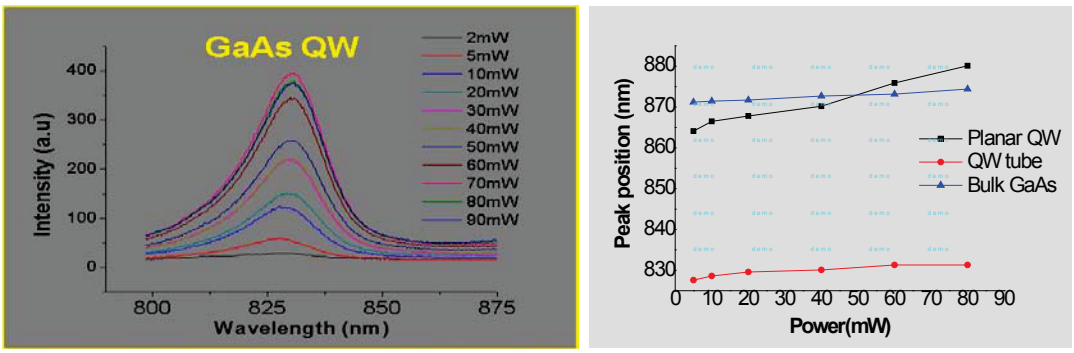

Figure 8 Power dependence of PL spectrum from a rolled-up GaAs QW tube that is 3 μm in diameter and 2.5 rotations for wall thickness. Structure is the same as Figure 4a.

Several mechanisms could be responsible for the broad emission (in contrast to mode-like peaks) from these GaAs quantum well tubes including leakage through substrate (tubes were not suspended), inhomogeneous broadening due to slight dispersion of tube diameters (for the clusters of tubes probed and along the axial direction from single tubes), absorption within the epitaxial structure (from layers that are not transparent to QW energy), and the lack of three-dimensional confinement as in quantum dots.

In addition to the intensity enhancement, another remarkable effect of rolling up the QW membranes is the strain induced peak shift. This can be seen clearly from Figure 9 that smaller tubes correspond to lower energy. This can be explained and fitted by bandgap shift due to the change of strain in the curved structure. To compensate for the partial relaxation of compressive strain in the InGaAs layer when the membrane is rolled up, the GaAs QW stack needs to be tensile strained near the InGaAs layer. By analyzing the strain distribution and calculating the amount of tensile strain the GaAs QW experiences, the amount of valence band splitting can be calculated. Shown in Figure 9 (right) are the

calculated vs experimental data and good agreement has been found. Our systematic study of this phenomenon is consistent with various literature results.[13] The implication of using curvature to change the band structure, thus effective mass and other associated properties is a new paradigm and could potentially lead to applications not only in optoelectronics but also in electronics.

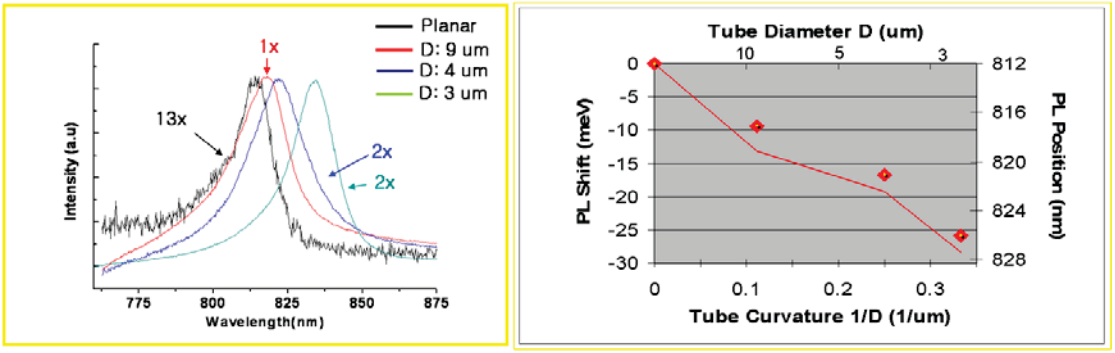

Figure 9 Effect of tube curvature on PL position. Left: PL spectra from QW tubes of various diameter, normalized in intensity with indicated intensity ratios, showing the red shift of peak energy with reducing tube diameter. Right: PL peak shift vs tube diameter plot where symbols are experimental data and lines are calculated data from strain induced bandgap shift model.

In summary, we have demonstrated the rolling process of strained epitaxial films upon releasing from the substrate. The formed tubular structure embedded with quantum confined light emitters in the ultra-thin tube walls show dramatic enhancement in intensity and reduction of bandgap as a function of tube curvature.

Xiuling Li acknowledges the support from NSF CAREER ECCS 07-47178 and DARPA YFA.

References

[1] Prinz, V. Y., Golod, S. V., Mashanov, V. I., and Gutakovsky, A. K., "Free-standing conductive GeSi/Si helical microcoils, micro- and nanotubes," *Compound Semiconductors 1999. Proceedings of the Twenty-Sixth International Symposium on Compound Semiconductors*, p. 203, 2000.

[2] Chun, I. S., Verma, V. B., Elarde, V. C., Kim, S. K., Zuo, J. M., Coleman, J. J., and Li, X., "InGaAs/GaAs 3D architecture formation by strain-induced self-rolling with lithographically defined rectangular stripe arrays " *Journal of Crystal Growth,* vol. 310, p. 2353, 2008.

[3] Chun, I. S. and Li, X., "Controlled assembly and dispersion of strain-induced InGaAs/GaAs nanotubes," *IEEE Transactions on Nanotechnology,* vol. 7, pp. 493-495, 2008.

[4] Brantley, W. A., "Calculated elastic constants for stress problems associated with semiconductor devices," *Journal of Applied Physics,* vol. 44, p. 534, 1973.

[5] Prinz, V. Y., Seleznev, V. A., Prinz, A. V., and Kopylov, A. V., "3D heterostructures and systems for novel MEMS/NEMS," *Science and Technology of Advanced Materials,* vol. 10, 2009.

[6] Strelow, C., Schultz, C. M., Rehberg, H., Welsch, H., Heyn, C., Heitmann, D., and Kipp, T., "Three dimensionally confined optical modes in quantum-well microtube ring resonators," *Physical Review B (Condensed Matter and Materials Physics),* vol. 76, pp. 1-5, 2007.

[7] Strelow, C., Rehberg, H., Schultz, C. M., Welsch, H., Heyn, C., Heitmann, D., and Kipp, T., "Optical microcavities formed by semiconductor microtubes using a bottlelike geometry," *Physical Review Letters,* vol. 101, p. 127403 (4 pp.), 2008.

[8] Li, F., Mi, Z., and Vicknesh, S., "Coherent emission from ultrathin-walled spiral InGaAs/GaAs quantum dot microtubes," *Optics Letters,* vol. 34, pp. 2915-2917, 2009.

[9] Fortuna, S. A., Wen, J., Chun, I. S., and Li, X., "Planar GaAs Nanowires on GaAs (100) Substrates: Self-Aligned, Nearly Twin-defect free, and transfer-printable," *Nano Letters,* vol. 8, p. 4421, 2008.

[10] Mendach, S., Songmuang, R., Kiravittaya, S., Rastelli, A., Benyoucef, M., and Schmidt, O. G., "Light emission and wave guiding of quantum dots in a tube," *Applied Physics Letters,* vol. 88, p. 111120, 2006.

[11] Yongfeng, M., Kiravittaya, S., Benyoucef, M., Thurmer, D. J., Zander, T., Deneke, C., Cavallo, F., Rastelli, A., and Schmidt, O. G., "Optical properties of a wrinkled nanomembrane with embedded quantum well," *Nano Letters,* vol. 7, pp. 1676-9, 2007.

[12] Hosoda, M., Kishimoto, Y., Sato, M., Nashima, S., Kubota, K., Saravanan, S., Vaccaro, P. O., Aida, T., and Ohtani, N., "Quantum-well microtube constructed from a freestanding thin quantum-well layer," *Applied Physics Letters,* vol. 83, pp. 1017-1019, 2003.

[13] Ohtani, N., Kishimoto, K., Kubota, K., Saravanan, S., Sato, Y., Nashima, S., Vaccaro, P., Aida, T., and Hosoda, M., "Uniaxial-strain-induced transition from type-II to type-I band configuration of quantum well microtubes," *Physica E (Netherlands)*, vol. 21, p. 732, 2004.